ORIGINAL PAPER

B. Lavina · L. Z. Reznitskii · F. Bosi

Crystal chemistry of some Mg, Cr, V normal spinels from Sludyanka (Lake Baikal, Russia): the influence of V^{3+} on structural stability

Abstract A suite of vanadian magnesiochromites from the Sludyanka metamorphic complex (South Lake Baikal, Russia) were investigated by means of X-ray single-crystal structural refinements and microprobe analyses. Various morphological types of Cr–V-bearing Mg spinels are located in calc–silicate metamorphic rocks, in an assemblage that also contains other Cr–V minerals such as escolaite–karelianite, uvarovite–goldmanite, Cr–V-bearing clinopyroxene, tourmaline, amphibole, mica, etc. Along the suite there is widespread V–Cr substitution ($0.14 \leq V^{3+} \leq 0.95$ afu, $1.02 \leq Cr^{3+} \leq 1.80$ afu), and minor, variable Al contents. The Mg content of slightly lesser than 1 afu, is almost constant. Cell parameters and octahedral bond distances increase with V^{3+}. Unexpectedly, the Mg–O tetrahedral bond distance also increases slowly with V^{3+}. This weak dragging effect contributes towards maintaining distortion of the oxygen array with respect to the ideal CCP, thus providing a shielding effect, which reduces V^{3+}–V^{3+} repulsion. This leads to the energetic stabilization of the structure, in spite of the increase of bond strain with increasing V^{3+} contents.

Keywords Spinel · Crystal chemistry · Magnesio-coulsonite · V-magnesiochromite · Sludyanka

B. Lavina (✉)
Dipartimento di Mineralogia e Petrologia,
Università di Padova, C.so Garibaldi 37,
I-35137 Padova, Italy
Tel: +39-49 8272032
Fax: +39-49 8272010
e-mail: barbara@dmp.unipd.it

L.Z. Reznitskii
The Siberian Division of Russian Academy of Sciences,
Institute of the Earth's Crust, Irkutsk, 664033 Russia
e-mail: garry@crust.irk.ru

F. Bosi
Dipartimento di Scienze della Terra,
Università di Roma 'La Sapienza', 00185 Roma, Italy
e-mail: ferdinando.bosi@uniroma1.it

Introduction

Multiple oxides with spinel-type structure may be described by the $^{IV}(A_{1-x}B_x)^{VI}(B_{2-x}A_x)O_4$ structural formula, where A and B are cations with variable valence and x is the inversion parameter. Normal spinels are those with $x = 0$, inverse spinels have $x = 1$. The structure is described generally as a cubic close packed (CCP) array of anions, with A and B cations distributed in one-eighth of all tetrahedral (T) and half of all octahedral (M) sites. The unit cell (lattice parameter a) is a face-centered cubic that contains 32 anions. Within the space group $Fd\bar{3}m$, the cations are fixed at special positions 8a (T) and 16d (M). Anions also occupy a special position, 32e, but with a variable fractional coordinate (u,u,u). With origin at center $\bar{3}m$, parameter u ranges from 0.24 to 0.27. The u value is an indicator of the regularity of the CCP, for ideal close-packed $u = 0.25$: the anions form a regular tetrahedron (8a point symmetry $\bar{4}3m$) and a regular octahedron (16d point symmetry $m3m$). Distortion of the CCP arises when $u \neq 0.25$: as u increases, oxygen is displaced along the [111] direction, causing a larger tetrahedral site at the expense of a smaller octahedral site. As the positions of cations A and B are fixed, the oxygen array expands (or contracts) around them, maintaining the same symmetry throughout. Similarly, the octahedron undergoes angular distortion and its symmetry degenerates to $\bar{3}m$ (trigonally distorted octahedron), whereas the tetrahedron is always regular.

The fractional coordinate is thus closely related to distortion of the CCP. The structure is rather rigid, with only two variable parameters, u and a, and the formal solution of all the geometrical equations is quite simple (Hill et al. 1979). Thus, the T–O and M–O bond distances can be used to calculate all the geometrical parameters, in particular u, using the following equation:

$$u = \frac{\frac{3(M-O)^2}{4(T-O)^2} - 2 + \sqrt{\frac{33(M-O)^2}{16(T-O)^2} - \frac{1}{2}}}{6\left[\frac{(M-O)^2}{(T-O)^2} - 1\right]} . \tag{1}$$

The strong preference of Cr^{3+} and V^{3+} for the octahedral site, due to their crystal-field stabilization energy, (CFSE) allows us to investigate how the structure of these normal spinels behaves with isomorphous replacement involving only the M site with the T site being filled by Mg alone.

V^{3+} is commonly present in spinels as a minor (or trace) element, since the CFSE contribution of 3d transition elements to the lattice energy is higher in the almost regular oxygen packing of these oxides, rather than in the more or less distorted silicates.

This is the first crystal-chemical study on natural high-V spinels. Previous works on the crystal chemistry of V in spinels were mainly concerned with synthetic compositions, which are very important for their electric and magnetic properties in materials science (see, for instance, Miyoshi et al. 2000; Liu et al. 2001).

We report here the results of crystal-chemical investigation by microprobe analysis and single-crystal structure refinement of a suite of natural spinels with the general formula $Mg(Cr_{2-x-y}V_xAl_y)O_4$, where $0.14 < x < 0.95$ and $0.02 < y < 0.09$.

Geological setting and occurrence of V-bearing spinels

The Sludyanka crystalline complex is situated on the southern shore of Lake Baikal, Russia, and belongs to the Central Asian foldbelt. The complex includes supracrustals, which are represented by intercalated high-grade gneiss, crystalline schist, marble and carbonate-silicate rocks. The complex underwent progressive granulite facies metamorphism ($T = 800–880 \,°C$, $P = 6–8$ kbar) at 480–490 Ma, and then partially retrogressed to conditions of amphibolite to epidote–amphibolite facies at 450–470 Ma.

The Cr–V mineral assemblage is related to certain lithological types of metamorphites, called quartz–diopside rock suites, derived from siliceous-dolomite sediments. According to the ratio between main rock-forming minerals (quartz, diopside, calcite), a series of petrographical types of diopside, quartz–diopside and carbonate–diopside rocks, diopside quartzite and calciphyre were recognized. Thin layers and lenses of Cr–V-bearing varieties sometimes occur irregularly within bends in the quartz–diopside rock suite. These varieties contain V-bearing spinels among an ample range of Cr–V silicates and opaque minerals (Reznitskii and Sklyarov 1996).

Three different forms of V-bearing spinels of interest are distinguished. The first is accessory magnesiochromite, present in practically any rock type. It forms euhedral and subhedral octahedral crystals 0.05–0.25 mm in size, included in quartz, calcite, Cr–V-diopside and some secondary minerals (Cr–V-tremolite, chlorite, muscovite). The assemblage also includes escolaite, V-escolaite, goldmanite–uvarovite, and sometimes Cr–V-tourmaline and natalyite-cosmochlor. The second type of spinel is found in quartz-free
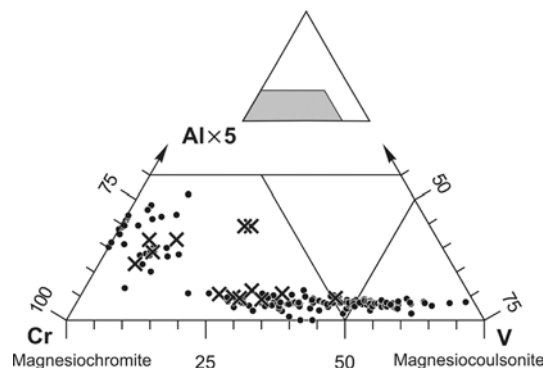

Fig. 1 Cr–V–Al ternary diagram, showing compositions of Sludyanka spinels. *Crosses* Compositions of spinels listed in Tables 2–4

diopside and carbonate–diopside rocks, sometimes containing small layers (from 0.2 to 3 cm) which consist of up to 50–60% spinel. The second type of spinel is also present as inclusions of euhedral crystals in Cr–V-bearing diopside and tremolite. However, the spinel inclusions may represent over 50% of the volume of the host minerals.

The composition of spinels of both types is identical, being magnesiochromite with some Al_2O_3 (in a range of 1.5–2.5 wt%) and V_2O_3. The concentrations of the latter vary more significantly, from 0.2–0.5 to 10–15 wt%, sometimes up to 20%. Spinels from quartz-bearing rocks often contain up to 1–1.6 wt% of SiO_2. Magnesiochromite is considered to be of primary (singranulite) paragenesis (Reznitskii et al. 1995a).

The third type of spinel has high V and belongs to the magnesiochromite–magnesiocoulsonite join (V_2O_3 from 20–25 to 50–55 wt%). It is rarely found in highly retrogressed rocks, and is composed of Cr–V-bearing tremolite with an admixture of diopside, calcite and quartz (Reznitskii et al. 1995b). The assemblage also includes karelianite, goldmanite, Cr-chlorite and Cr-muscovite. Besides these minerals, there is always some admixture of an unnamed opaque V–Cr–Mg mineral. This unnamed mineral has a spinel-like structure, but differs from spinels by its formal valences of cations and site occupancies (work in progress). It is believed that the third type of spinel partially recrystallized during retrograde metamorphism and that it occurs in two generations. The V-magnesiochromite (V_2O_3 20–30 wt%) of euhedral crystals suggested that it belongs to primary paragenesis, but the magnesiocoulsonite of anhedral grains formed during retrograde metamorphism (at about 550–600 °C).

The overall range of compositions of the magnesochromite–magnesiocoulsonite series from the Sludyanka rocks and studied spinels is shown in Fig. 1.

Experimental

Spinel crystals were picked from two series of samples. Low-V spinels (VRL2a,b,c,d) are of type 2 (rock-forming), whereas high-V

spinels, called V-magnesiochromite, are of type 3 (VRL1a,b,d,e,p,r primary generation, and VRL 3a,b,c second generation).

Several crystals were tested and selected on the basis of diffraction quality and cell-parameter variations, obtaining 13 crystals with a ranging from 8.33 to 8.38 Å. Measurements were performed with two four-circle single-crystal diffractometers, Siemens P4 and Stadi4 CCD, equipped with an area detector. Experimental conditions are summarized in Table 1. Both instruments used monochromatized Mo-Kα radiation. Unit-cell parameters for data collection performed with Siemens P4 were obtained after centering on both sides of the direct beam 12 independent reflections and their Friedel pairs, chosen in the $83° < 2\theta < 92°$ range, with MoKα_1 radiation ($\lambda = 0.70930$ Å). All reflections with I > 4σ(I) were used for unit-cell determination for data collections performed with the Stadi4 CCD diffractometer. Measurements of the same crystal with the two instruments matched all the structural parameters within two standard deviations.

The Stadi4 CCD was also used to collect the diffraction intensities of a polycrystalline grain (sample VRL3c). This was necessary because spinels with the highest V contents, even in fragments as small as 50 μ, were not found as single crystals. The collected data were indexed by three distinct lattices, with very similar cell parameters. The lattice with the most intense peaks was used for structural analyses. Due to some unavoidable overlapping, the obtained data have higher standard deviations than those from single-crystal grains, but they are in any case satisfactory.

Structural refinements were performed with the SHELXL-97 program (Sheldrick 1997) without chemical constraints. Variable parameters were scale factor, oxygen coordinate (u), T and M occupancies, displacement factors and isotropic secondary extinction coefficient. The ionization level of the scattering curves was selected in order to obtain the best values of conventional agreement factors over all sin θ/λ intervals, and the minimum difference between calculated and observed F(222), a structure factor very sensitive to the occupancies and ionization level of M and oxygen sites (Della Giusta et al. 1986). Results are listed in Table 2, where only the U_{11} values are reported, as the off-diagonal terms are very small and close to their standard deviation, which is usual for the spinel structure.

Each crystal was then analyzed with a Cameca-Camebax microprobe (WDS method) at 15 kV, 15 nA, with the PAP data-reduction program. Results are listed in Table 3. Synthetic oxide standards (MgO, FeO, MnO, ZnO, NiO, CuO, Al_2O_3, Cr_2O_3, V_2O_3, TiO_2, SiO_2) were used. Precision for major elements was usually within 1% of the actual amounts present; that of minor elements was close to 5%. Up to 20 point analyses were performed on each sample, showing satisfactory homogeneity and no evidence of zoning for most samples. Sample VRL3c shows the largest sigma

for Cr and V, which is probably due to the fact that it is not a single crystal, as already mentioned.

Results and conclusions

Bulk chemistry

The investigated spinels belong to the magnesiochromite–magnesiocoulsonite join, with $0.14 \leq V^{3+} \leq 0.95$ afu and $1.02 \leq Cr^{3+} \leq 1.80$ afu. These cations are partly, and randomly, substituted by $0.02 \leq Al \leq 0.09$ afu. Divalent cations are essentially Mg, in amounts greater than 0.97 afu. Each other element, Fe^{2+}, Mn^{2+}, and Zn, is less than 0.02 afu. Si, Cu, and Ti are lower than the detection limit; no other elements were detected by the EDS method. Vanadium may take on several valence states, but we obtained consistent crystal-chemical formulas by considering it as solely trivalent.

Structural parameters

Along the join, the cell parameter a increases from 8.333 to 8.380 Å, and is closely related (Fig. 2) to an increase in M–O bond distance from 1.992 to 2.007 Å. The T–O distance is not constant, but shows a slight increase from 1.966 to 1.974 with V^{3+} (Fig. 3a). The almost constant u observed in the Sludyanka V-spinels depends on the fact that the M–O bond distance increases due to V $\rightarrow$ Cr substitution is associated with the small but definite T–O increase. This, in the absence of significant isomorphous substitutions in the T site, must be due to a small "dragging effect" of the M site on the T site, similar to that already demonstrated for octahedral Fe^{3+} and Ni^{2+} (Lavina et al. 2002).

The mean atomic numbers of both tetrahedral and octahedral sites remain virtually unchanged all along the join, with values close to 12.1 and 23.4, respectively,

Table 1 Experimental conditions for X-ray data collection, data reduction, and structural refinement.

Unit cell parameter determination	
Radiation	Mo–Kα1 (0.70930 Å)
Reflection used (Siemens P4)	12(Friedel pairs on both $+2\theta$ and -2θ)
2θ range	83–92°
Reflection used (Stadi4CCD)	Reflections with I > 10σ(I)
2θ range	10–90°
Temperature	296 K
Diffraction intensity collection	
Radiation	Mo–Kα (0.71073 Å)
Monochromator	High crystallinity graphite crystal
2θ range	3–95°
Reciprocal space range	$0 \leq$ h,k,l ≤ 17
Scan method	ω
Temperature	296 K
Data reduction	
Corrections	Lorentz, polarization
Absorption correction (Siemens P4)	Semi-empirical, 13 Ψ-scans (0–95° 2θ)
Absorption correction (Stadi4CCD)	Optimized shape
Set of measured reflections	707—717
Set of unique reflections	165–169{I > 2σ(I)}

Table 2 Structural data obtained for V-magnesiochromite. *man* Mean atomic number; *ext* isotropic secondary extinction coefficient; *R(int)* disagreement factor between equivalent reflections (%); *R* disagreement factor (%) Instrument (1) Siemens P4, (2) Stadi4 CCD

Sample Instrument	VRL2a (2)	VRL2d (2)	VRL2c (2)	VRL2b (1)	VRL1r (1)	VRL1p (1)	VRL1a (1)	VRL1b (1)	VRL3a (2)	VRL1d (1)	VRL1e (1)	VRL3b (2)	VRL3c (2)
a (Å)	8.3367(6)	8.3431(4)	8.3334(7)	8.3369(5)	8.3584(3)	8.3479(3)	8.3613(3)	8.3511(2)	8.3664(4)	8.3604(3)	8.3629(4)	8.3686(6)	8.3800(6)
u	0.26114(9)	0.26123(7)	0.2614(1)	0.2613(1)	0.26091(6)	0.26117(7)	0.26092(6)	0.26105(6)	0.26089(7)	0.26096(8)	0.26097(6)	0.261(1)	0.2610(3)
T–O(Å)	1.966(1)	1.969(1)	1.968(1)	1.967(2)	1.9676(9)	1.969(1)	1.9684(9)	1.968(1)	1.969(1)	1.969(1)	1.9695(9)	1.971(1)	1.974(4)
M–O(Å)	1.995(1)	1.996(1)	1.992(1)	1.995(1)	2.003(1)	1.998(1)	2.003(1)	2.000(1)	2.005(1)	2.003(1)	2.003(1)	2.004(1)	2.007(2)
$R(int)$	2.43	3.0	5.2	3.7	2.31	2.80	2.27	2.07	2.7	2.5	2.34	5	14
$R(all)$	2.38	2.0	3.3	3.22	1.58	1.70	1.52	1.55	1.9	1.90	1.54	2	5
$wR2$	3.07	2.6	3.9	6.24	2.82	3.74	3.12	2.91	2.7	4.53	3.26	3.2	9.5
Goof	0.83	0.75	0.72	1.01	1.13	1.12	1.12	0.97	0.81	1.14	1.11	0.80	0.87
Ext	0.0166(7)	0.014(1)	0.0163(9)	0.016(2)	0.0102(6)	0.037(2)	0.013(1)	0.0178(7)	0.0116(4)	0.012(1)	0.010(1)	0.0043(3)	0.001(1)
man_T	12.0(1)	12.1(1)	12.0(1)	12.0(2)	12.1(1)	12.3(1)	12.1(1)	12.3(1)	12.1(1)	12.0(2)	12.1(1)	11.9(1)	12.6(3)
man_M	23.1(1)	23.5(1)	23.9(2)	23.6(3)	23.3(2)	23.2(2)	23.5(2)	23.4(1)	23.4(1)	23.4(2)	23.4(2)	23.4(1)	24.1(4)
man_{TQT}	58.2	59.2	59.8	59.2	58.6	58.7	59.2	59.0	58.9	58.7	58.9	58.7	60.8
U_{11O}(Å²*10⁻⁴)	49(2)	54(2)	52(4)	86(4)	60(2)	618(2)	52(2)	44(2)	55(2)	56(2)	55(2)	61(3)	57(8)
U_{11T}(Å²*10⁻⁴)	48(3)	59(3)	51(5)	81(4)	58(2)	60(2)	48(2)	42(2)	54(2)	50(2)	51(2)	60(1)	60(8)
U_{11M}(Å²*10⁻⁴)	36(1)	47(1)	51(1)	74(1)	46(1)	47(1)	38(1)	31(1)	43(1)	39(1)	39(1)	53(1)	59(2)

Table 3 Chemical compositions

	Sample	VRL2a	VRL2d	VRL2c	VRL2b	VRL1r	VRL1p	VRL1a	VRL1b	VRL3a	VRL1d	VRL1e	VRL3b	VRL3c
Wt%														
	MgO	20.9(2)	21.2(2)	20.9(3)	20.4(2)	20.8(2)	20.8(2)	20.8(3)	20.8(2)	20.8(1)	20.9(2)	20.9(2)	20.8(2)	20.9(1)
	FeO	0.2(1)	0.11(3)	0.07(4)	0.11(4)	0.35(6)	0.68(6)	0.36(7)	0.37(6)	0.17(4)	0.16(5)	0.38(5)	0.33(4)	0.07(3)
	MnO	0.00(4)	0.07(2)	0.00(0)	0.08(6)	0.12(4)	0.14(4)	0.11(4)	0.11(5)	0.07(2)	0.11(5)	0.12(5)		
	ZnO	0.31(7)	0.3(1)	0.25(4)	0.21(9)	0.21(6)	0.22(8)	0.20(8)	0.21(7)	0.40(9)			0.3(1)	0.63(4)
	Al_2O_3	1.4(1)	2.1(2)	1.7(1)	2.1(1)	0.71(4)	2.42(7)	2.31(3)	2.3(3)	0.52(4)	0.61(6)	0.51(2)	0.62(3)	0.50(2)
	V_2O_3	5.6(4)	5.8(6)	7.3(7)	10(1)	20.0(1)	20.8(2)	22(1)	21.6(2)	22.2(8)	24.8(7)	27(1)	29(1)	37(2)
	Cr_2O_3	71.9(2)	70.8(9)	69.5(9)	66(2)	58(1)	55.5(7)	54(1)	54.2(4)	55.4(9)	53(1)	52(1)	49(1)	40(2)
	Total	100.31	100.38	99.72	98.90	100.19	100.56	99.78	99.59	99.56	99.58	100.91	100.05	99.10
Cations per 4 oxygen														
T site	Mg	0.990(7)	1.00(1)	0.99(1)	0.97(2)	0.99(1)	0.979(9)	0.99(1)	0.987(8)	0.99(1)	0.99(1)	0.99(1)	0.99(1)	1.00(1)
	Fe^{2+}	0.005(2)	0.003(1)	0.002(1)	0.003(1)	0.009(2)	0.018(2)	0.010(2)	0.010(2)	0.005(1)	0.004(1)	0.010(1)	0.009(1)	0.002(1)
	Mn^{2+}		0.002(1)		0.002(2)	0.003(1)	0.004(1)	0.003(1)	0.003(1)	0.002(1)	0.003(1)	0.003(1)		
	Zn	0.007(2)	0.008(2)	0.006(1)	0.005(2)	0.005(1)	0.005(2)	0.005(1)	0.005(2)	0.008(2)			0.008(2)	0.015(1)
M site	Al	0.053(4)	0.077(7)	0.064(4)	0.078(4)	0.027(1)	0.090(3)	0.086(2)	0.09(1)	0.020(1)	0.023(2)	0.019(1)	0.023(1)	0.019(1)
	V	0.142(9)	0.15(1)	0.19(1)	0.26(2)	0.511(5)	0.524(5)	0.55(2)	0.551(5)	0.57(2)	0.64(1)	0.68(2)	0.74(2)	0.95(4)
	Cr	1.804(9)	1.77(1)	1.75(1)	1.67(3)	1.46(1)	1.38(1)	1.36(2)	1.360(9)	1.40(2)	1.34(2)	1.30(2)	1.23(2)	1.02(4)
	Total	3.001	3.010	3.002	2.988	3.005	3.000	3.004	3.006	2.995	3.000	3.002	3.000	3.006

clearly suggesting only almost iso-electronic substitutions.

The substitution of V^{3+} for Cr^{3+} is responsible for the M–O increase, as shown in Fig. 3b, where the dotted lines represent M–O variations with Cr–V substitution calculated for $^{VI}Al = 0$ and $^{VI}Al = 0.1$ afu (all calculations use the optimized bond distances from Lavina et al. 2002). The amounts of Al, not related to other cations, explain the irregularities in the trend of the M–O bond length.
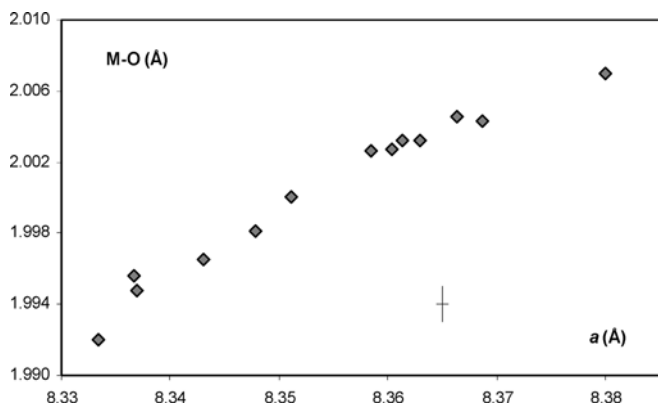

Fig. 2 Relation between structural parameter M–O and *a*. *Cross Mean standard deviation*
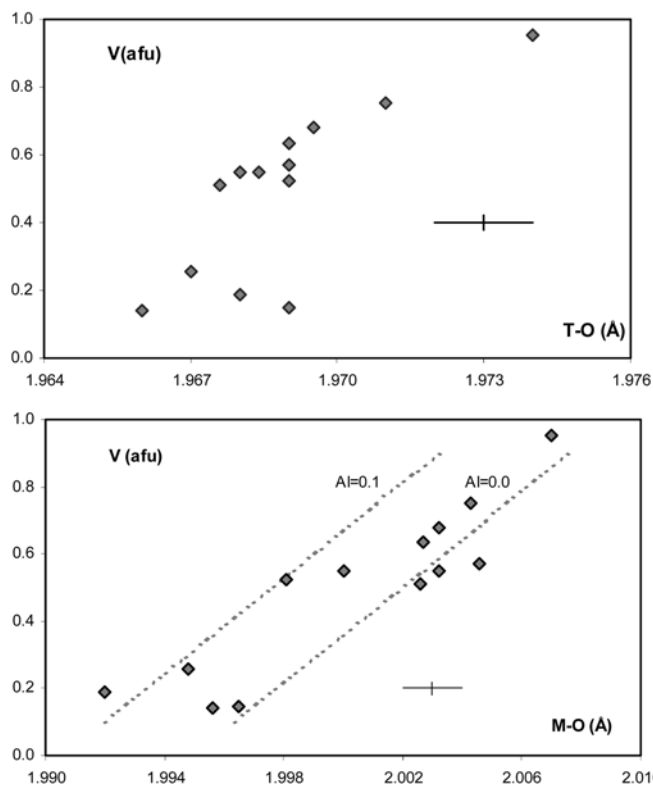
Fig. 3a, b Variations in T–O (**a**) and M–O (**b**) bond distances with vanadium. *Dotted lines* in **b** calculations for $^{VI}Al = 0$ and $^{VI}Al = 0.1$; *crosses* mean standard deviations

Within this join, rather different compositions such as VRL2a and VRL2b give equal values for *a* and *u*, since the effect of the large $^{VI}V^{3+}$ cation is fully counterbalanced by small amounts of the very small $^{VI}Al^{3+}$ cation. Figure 3b shows that the Al–Cr replacement causes a decrease in M–O about three times greater than the increase caused by the V–Cr substitution in equal amounts.

Calculation of the cation distribution by means of the structure modeling adopted by Lavina et al. (2002) confirmed normal cation distribution all along the join, with no evidence of intracrystalline disordering, isomorphous replacement involving only the octahedral site.

The possibility of the presence of mixed-valence vanadium in our samples was also evaluated. V^{2+} was excluded because it would require a M–O bond length longer than the measured one. Furthermore, the paragenesis includes other oxides with V^{4+} and V^{5+}. The presence of appreciable amounts of V^{4+} was excluded, since it would have caused a cation-deficient crystal-chemical formula, whereas our structural refinements indicate full occupancy of both sites; it would also have appreciably decreased the M–O bond length. A satisfactory agreement between observed and calculated bond lengths is only obtained by assuming that vanadium is essentially V^{3+}.

Properties of the M site

A comparison of this fully ordered suite with data on normal or almost normal Mg-spinels allows us to describe some features of the M-site chemical bond in the $Mg (Al, Cr, V)_2O_4$ system. We considered the literature data of a suite of $Mg(Al,Cr)_2O_4$ spinels with $0.02 < Cr < 0.25$ afu (inversion degree close to 0.1; Lavina et al. 2003), the data of synthetic $MgCr_2O_4$ (O'Neill and Dollase 1994) and MgV_2O_4 spinel (Mamiya and Onoda 1995). The data for the three end members of the system, with $MgAl_2O_4$ ideally fully normal, were calculated from bond distances. Synthetic and theoretical $MgCr_2O_4$ coincide in their structural values.

The T–O bond distance of synthetic MgV_2O_4 (T–O = 1.971 Å) is substantially greater than the optimized tetrahedral Mg-O (1.966 Å). This fact confirms the presence of a dragging effect of $^{VI}V^{3+}$ which lengthens T–O. Consequently, the actual cell edge is larger than the calculated one (8.431 as opposed to 8.410 Å). This effect of $^{VI}V^{3+}$ is also confirmed by the data of Mamiya and Onoda (1995) of synthetic ZnV_2O_4. Also in this case, the experimental cell edge (8.435 Å) is definitely greater than that calculated from bond distances (8.401 Å).

Bond valences were calculated for all these samples (Table 4) using the equation proposed by Brown and Altermatt (1985):

$$S_{ij} = \exp\left(\frac{R_0 - R_{ij}}{0.37}\right) ,$$

Table 4 Bond valence calculations for V-magnesiocoulsonite from Sludyanka, and for other almost normal spinels for comparison

Samples	S_{OT}^{a}	S_{OM}	BVS_{T}^{b}	BVS_{M}	GII^{c}
VRL2a	0.479	0.479	1.915	2.875	0.098
VRL2d	0.475	0.477	1.901	2.862	0.109
VRL2c	0.475	0.483	1.899	2.897	0.089
VRL2b	0.476	0.481	1.903	2.885	0.094
VRL1r	0.477	0.476	1.908	2.856	0.111
VRL1p	0.476	0.479	1.904	2.874	0.101
VRL1a	0.476	0.473	1.904	2.837	0.123
VRL1b	0.477	0.477	1.907	2.864	0.106
VRL3a	0.475	0.474	1.899	2.846	0.119
VRL1d	0.475	0.478	1.901	2.865	0.107
VRL1e	0.475	0.478	1.898	2.866	0.107
VRL3b	0.472	0.477	1.888	2.861	0.113
VRL3c	0.468	0.476	1.873	2.856	0.120
Samples from Lavina et al. (2003)					
T4–2b	0.505	0.488	2.020	2.930	0.048
T4–2f	0.505	0.488	2.020	2.930	0.048
T4–2g	0.504	0.488	2.015	2.930	0.048
T4–2c	0.504	0.488	2.016	2.928	0.049
T4–2i	0.503	0.488	2.011	2.928	0.049
T4–2L	0.503	0.487	2.012	2.924	0.050
T4–2e	0.500	0.488	1.999	2.928	0.052
Mamiya and Onoda (1995)					
MgV_2O_4	0.471	0.464	1.885	2.785	0.160
Theoretical normal spinel					
$MgAl_2O_4$	0.478	0.499	1.913	2.996	0.038
$MgCr_2O_4^{d}$	0.478	0.481	1.913	2.884	0.092
MgV_2O_4	0.478	0.470	1.913	2.823	0.131

[a] S bond valence (vu)
[b] BVS bond valence sum (ΣS)
[c] GII global instability index
[d] Theoretical and synthetic terms have the same values

where R_{ij} is the length of the bond between atoms i and j, S_{ij} its bond valence, and R_0 an empirical parameter characteristic of the atom pair forming the bond. We recall that in spinel structure tetrahedron is perfectly regular and octahedron can be only tetragonally distorted, then the four tetrahedral and six octahedral bond distances are equal, so S_{OT} is the bond valence of the T site and S_{OM} is that of the M site.

In structures with unstrained bonds, the sum of the bond valence (BVS) around each atom is equal to the atomic valence: $\Sigma S = V$ (valence sum rule). In theoretical end members, where the atomic valence of the M site is always $3+$, the values of BVS of the M site (BVS_M) decrease from 3.00 vu (valence units) for fully normal $MgAl_2O_4$ to 2.88 vu for $MgCr_2O_4$ to 2.82 vu for MgV_2O_4, the two natural suites present BVS_M intermediate to those of the relative end members (Table 4). The deviation of the bond valence sum (BVS) from the atomic valence is due to steric effects (Brown 1992), which are related to the way in which the bonds are strained in a crystal. An estimate of the degree of strain is given by the global instability index GII (Salinas-Sanchez et al. 1992):

$$GII = \sqrt{\frac{\sum_i \left(\sum_j S_{ij} - V_i \right)^2}{N}} \, ,$$

where N is the number of atoms in the asymmetric units.

The GII evaluates the extent to which the valence sum rule is violated. Brown (2002) pointed out that values of GII larger than about 0.05 vu are indicative of stress, which produces intrinsic strain in the structure (lattice-induced strain). Crystals with GII $\gg$ 0.2 vu are generally unstable. The GII values for samples in the $Mg(Al,Cr,V)_2O_4$ system show that crystals with $^{VI}Cr^{3+}$, and especially those with $^{VI}V^{3+}$, are subject to steric effects (tensile bond strain). ^{IV}Mg is also underbonded and consequently also shows tensile bond strain.

The small crosses linking parameter u and GII in Fig. 4 show theoretical behavior in the $MgAl_2O_4$–$MgCr_2O_4$ and $MgCr_2O_4$–MgV_2O_4 joins. In this join, the T site is always occupied by Mg, so that the calculated T–O is constant (1.966 Å), since the model does not consider any dragging effect for this composition; moreover, the atomic valence is $2+$. The u and GII values of the intermediate terms of joins depend on the M–O change, that is, on the progressive $^{VI}Al \rightarrow$ $^{VI}Cr^{3+} \rightarrow$ $^{VI}V^{3+}$ substitution. The octahedral bond distance was calculated as the linear contribution of each site cation (X_i) multiplied by its specific bond distance according to: M–O = $^{VI}(Al–O)$ X_{Al} + $^{VI}(Cr–O)$ X_{Cr3+} + $^{VI}(V–O)$ X_{V3+}. The negative correlation between u and GII shows that in this system lattice distortion removes bond strain and therefore relaxes the structure: ^{VI}Al does not induce stress in the structure of spinel s.s—which shows the highest u value—unlike $^{VI}Cr^{3+}$ and $^{VI}V^{3+}$. The position of the $Mg(Al, Cr)_2O_4$ series (stars in Fig. 4) is out of the theoretical trend of fully normal spinels, due to their inversion degree, which
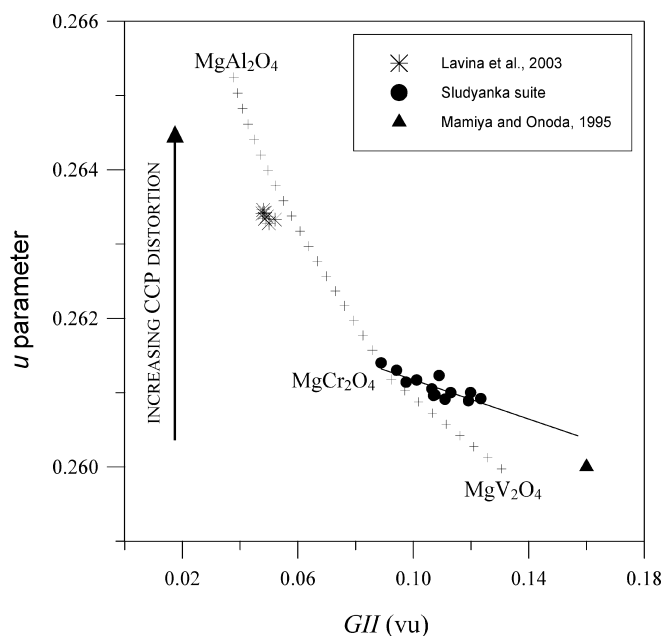

Fig. 4 u vs. GII. The *crosses* are the theoretical trend for normal spinels $Mg(Al,Cr,V)_2O_4$. The *solid line* is linear regression ($R = -0.83$) for the Sludyanka suite

causes a decrease in u with respect to fully ordered $MgAl_2O_4$. In the $Mg(Cr, V)_2O_4$ series, samples progressively shift from theoretical behavior towards larger u values with increasing V^{3+}. We emphasize that the GII of experimental MgV_2O_4 is definitely higher than that of theoretical MgV_2O_4, due to higher T–O bond distances. Considering an uncertainty of about 0.001 for the u parameter determined by Mamiya and Onoda (1995), the location of MgV_2O_4 in Fig. 4 is in satisfactory agreement with the trend of the Sludyanka suite, whose trend, for $V^{3+} = 2$ afu, predicts a coordinate of about 0.2605, not very far from the 0.260 reported by Mamiya and Onoda (1995).

The influence of the Jahn–Teller distortion in V-magnesiochromite crystals was considered negligible. In fact, although the theory predicts the Jahn–Teller effect for $^{VI}V^{3+}$, it is of little importance, since the electrons in the orbital t_{2g} are located in the region between the ligands and thus do not point directly to the ligand. Furthermore, in spinel structure, all octahedral bond distances are equal due to symmetry constraint; the possible Jahn–Teller effect has dynamic behavior and the electronic asymmetry of $^{VI}V^{3+}$ is not large enough to cause distortion in M–O bond distances. The extent of the amount by which electronic effects change bond distances is given by the BSI (bond strain index; Brown 2002). BSI > 0.05 vu are characteristic of structures with electronically induced distortions. The values of BSI calculated in the V–magnesiocromite samples are less than 0.03 vu, so that strain introduced by electronic asymmetry can be excluded.

The observed u values, greater than those calculated with constant T–O (crosses in Fig. 4), suggest that this is the way in which the structure maintains consistent distortion. In the V–spinels from Sludyanka, the T–O bonds are strained in order to increase u. This leads to a decrease in the octahedral shared edge, thus providing a shielding effect which reduces V^{3+}–V^{3+} interaction. Preliminary computations performed following Della Giusta and Ottonello (1993) show that this leads to a decrease in the Gibbs free energy by about 10 KJ mol^{-1}, due to the decrease in repulsive energy which is definitely larger than the corresponding increase in Coulombic energy.

This behavior of the structure allows the values of the oxygen coordinate to remain greater than 0.26, which seems to be the minimum reached by normal spinels containing divalent and trivalent cations.

The great increase in GII with increasing V^{3+} contents may explain the difficulties in finding single crystals with high V contents, although single-spot analyses in Sludyanka samples showed V contents as high as 1.42 afu (V_2O_3 55.88 wt).

References

Brown ID (1992) Chemical and steric constraints in inorganic solids. Acta Crystallogr (B) 48: 553–572

Brown ID (2002) The chemical bond in inorganic chemistry: the bond valence model. Series: International union of crystallography monographs on crystallography, no. 12. Oxford University Press, 288 pp

Brown ID, Altermatt D (1985) Bond-valence parameters obtained from a systematic analysis of the inorganic crystal structure database. Acta Crystallogr (B) 41: 244–247

Della Giusta A, Ottonello G (1993) Energy and long-range disorder in simple spinels. Phys Chem Miner 20: 228–241

Della Giusta A, Princivalle F, Carbonin S (1986) Crystal chemistry of natural Cr-bearing spinels with $0.15 \leq Cr \leq 1.07$. N J Miner Abh 155: 319–330

Hill RJ, Craig JR, Gibbs GV (1979) Systematics of the spinel structure type. Phys Chem Miner 4: 317–339

Lavina B, Koneva A, Della Giusta A (2003) Cation distribution and cooling rates of Cr-substituted Mg–Al spinel from Olkhon metamorphic complex, Russia. Eur J Miner 15: 435–441

Lavina B, Salviulo G, Della Giusta A (2002) Cation distribution and structure modelling of spinel solid solutions. Phys Chem Miner 29: 10–18

Liu RS, Cheng YC, Gundakaram R, Jang LY (2001) Crystal and electronic structures of inverse spinel-type LiNiVO$_4$. Mat Res Bull 36: 1479–1486

Mamiya H, Onoda M (1995) Electronic states of vanadium spinels MgV_2O_4 and ZnV_2O_4. Solid State Comm 95: 217–221

Miyoshi K, Ihara M, Fujiwara K, Takeuchi J (2000) Magnetic phase transitions in the vanadium spinel system (Li_xMn_{1-x})-V_2O_4. Physica (B) 281–282: 30–31

O'Neill HSC, Dollase WA (1994) Crystal structures and cation distributions in simple spinels from powder XRD structural refinements: $MgCr_2O_4$, $ZnCr_2O_4$, Fe_3O_4 and the temperature dependence of the cation distribution in $ZnAl_2O_4$. Phys Chem Miner 20: 541–555

Reznitskii LZ, Sklyarov EV (1996) Unique Cr–V mineral association in metacarbonate rocks of the Sludyanka, Russia. 30th Int Geol Congr Beijin, China. Abstr 2–3: 446

Reznitskii LZ, Sklyarov EV, Nekrasova EA, Ushchapovskaya ZF (1995a) Magnesiochromite in metacarbonate rocks of the Sludyanka Group (South Baikal region). Doklady Acad Sci (Russia), Vol 343. 1: 87–90

Reznitskii LZ, Sklyarov EV, Ushchapovskaya ZF (1995b) Magnesiocoulsonite MgV_2O_4-a new mineral species in the spinel group. Proc Russian Mineralogical Society 124(4): 91–98

Salinas-Sanchez A Garcia-Muñoz JL, Rodriguez-Carvajal J, Saez-Puche R, Martinez JL (1992) Structural characterization of R_2BaCuO_5 (R = Y, Lu, Yb, Tm, Er, Ho, Dy, Gd, Eu and Sm) oxides by X-ray and neutron diffraction. J Solid State Chem 100: 201–211

Sheldrick GM (1997) SHELXL-97, a program for crystal structure refinement. University of Göttingen, Germany